The Meteoritical Society

Meteoritics & Planetary Science 1–13 (2016)
doi: 10.1111/maps.12666

Gas/solid carbon branching ratios in surface-mediated reactions and the incorporation of carbonaceous material into planetesimals

Joseph A. NUTH[1*], Natasha M. JOHNSON[2], Frank T. FERGUSON[2,3], and Alicia CARAYON[2,4]

[1]Solar System Exploration Division, Code 690, NASA Goddard Space Flight Center, Greenbelt, Maryland 20771, USA
[2]Astrochemistry Laboratory, Code 691, NASA Goddard Space Flight Center, Greenbelt, Maryland 20771, USA
[3]Chemistry Department, The Catholic University of America, Washington, D.C. 20064, USA
[4]International Space University, Strasbourg Central Campus, 1 Rue Jean-Dominique Cassini, 67400 Illkirch-Graffenstaden,France
[*]Corresponding author. E-mail: joseph.a.nuth@nasa.gov

(Received 31 August 2015; revision accepted 17 March 2016)

Abstract–We report the ratio of the initial carbon available as CO that forms gas-phase compounds compared to the fraction that deposits as a carbonaceous solid (the gas/solid branching ratio) as a function of time and temperature for iron, magnetite, and amorphous iron silicate smoke catalysts during surface-mediated reactions in an excess of hydrogen and in the presence of N_2. This fraction varies from more than 99% for an amorphous iron silicate smoke at 673 K to less than 40% for a magnetite catalyst at 873 K. The CO not converted into solids primarily forms methane, ethane, water, and CO_2, as well as a very wide range of organic molecules at very low concentration. Carbon deposits do not form continuous coatings on the catalytic surfaces, but instead form extremely high surface area per unit volume "filamentous" structures. While these structures will likely form more slowly but over much longer times in protostellar nebulae than in our experiments due to the much lower partial pressure of CO, such fluffy coatings on the surfaces of chondrules or calcium aluminum inclusions could promote grain–grain sticking during low-velocity collisions.

INTRODUCTION

Carbonaceous dust and silicate grains are intimately mixed in the interstellar medium (Mathis et al. 1977; Draine and Lee 1984). Prior to being incorporated into new protostars, the association of carbonaceous materials and silicates becomes even more intimate through the formation of carbonaceous coatings on the dust in giant molecular clouds (Sandford 2005). Until recently, there has been little consideration of exposing such a mixture to conditions in the evolving nebular environment. It has been estimated (Boynton 1985) that more than 95% of all presolar silicates were vaporized or melted in the primitive solar nebula. This implies that at least 95% of the presolar carbon dust was also destroyed (converted into CO or CO_2) during these same high-temperature events. Yet, solar system bodies are not greatly depleted in carbon and therefore at least one mechanism must be available in nature to convert highly volatile CO or CO_2 into carbonaceous solids that can then be accreted by growing planetesimals.

Studies of the catalytic activity of pre-existing interstellar grain surfaces or of grains formed in situ in the protosolar nebula are not new (Fegley and Hong 1998; Fegley 1999; Ferrante et al. 2000) and have generally focused on the formation of organic compounds found in meteorites, yet much more work on such processes is needed to complement and extend the pioneering work of Anders and his associates on the products of Fischer-Tropsch-type reactions in the nebula (for reviews see Anders et al. 1974; Hayatsu and Anders 1981; Kerridge 1989). Our interest in such processes has been to address other aspects of nebular chemistry. For example, we have suggested (Nuth et al. 2014) that Fischer-Tropsch-type surface-mediated reactions could convert the CO or CO_2 produced in high-temperature nebular events back into carbonaceous solids that could then be incorporated into planetesimals and that this same mechanism may also trap planetary noble gases into such solids (Nuth et al. 2010a).

We are not claiming here that surface-mediated reactions constitute the single—or even the most

important—mechanism that forms the full distribution of organic molecules in asteroids or comets or that are found in meteorites or IDPs. There are many different processes that can be important sources for particular compounds in many different meteorite types (Kerridge 1999). However, we do believe that surface-mediated reactions are a very efficient mechanism for converting nebular CO or CO_2 into solid carbonaceous materials. Such solids should be easy to incorporate into planetesimals and these carbonaceous grains could then serve as the feedstock that is transformed by various thermal or hydrothermal processes on parent bodies into the myriad organic molecules found in natural sources.

In addition, while we use various industrial reactions as models of nebular processes, e.g., the Fischer-Tropsch reaction: $CO + 3H_2 => CH_4 + H_2O$; the Haber-Bosch reaction: $N_2 + 3H_2 => 2NH_3$; the water-gas shift reaction: $CO + H_2O => CO_2 + H_2$; or the Boudouard reaction: $2CO => CO_2 + C_{solid}$, natural reactions on grain surfaces in protostellar nebulae are much more complex. For this reason, it can be extremely misleading to discuss a specific model reaction in isolation when describing natural reactions that might occur on the surfaces of grains in the solar nebula. Hereafter we will simply discuss measurements of *surface-mediated reactions*.

In our simple experimental system, starting with a mixture of $CO + N_2 + H_2$, we find a wealth of products including CH_4, CO_2, H_2O, C_2H_6, alkanes, aromatics, nitriles, amines, aldehydes, ketones, PAHs, and kerogens, among others. The specific ratios of this wide range in natural products depend on time, temperature, pressure, the catalyst used in the experiment, and the previous reaction history of the system (Hill and Nuth 2003; Gilmour et al. 2002). In the more complex and continuously changing environment of a protostellar nebula, an even more diverse set of products might be expected from reactions on grain surfaces. In what follows we present the first measurements of the trends we have observed using very simple analogs of natural surface-mediated reactions in the laboratory using both "normal" mineral catalysts such as iron and magnetite, both of which are found in meteorite matrices (Huss et al. 1981) as well as more unusual catalysts such as highly amorphous iron silicate smokes that serve as analogs for silicate condensates that may have formed in the nebula (Nuth et al. 2002).

EXPERIMENTAL METHODOLOGY

We recently began a series of experiments to quantitatively measure the gas/solid product ratio for surface-mediated processes as a function of catalyst, time, run number, and temperature. While we performed experiments using iron and magnetite powders as well as amorphous iron silicate smokes, the majority of these experiments were performed using magnetite as the catalyst. Magnetite was selected as the primary catalyst for these experiments because it was both abundant in the solar nebula (Huss et al. 1981) and is readily available commercially in well-defined particle sizes and purities, making our experiments easy to duplicate. For the current set of experiments, we used 325 mesh magnetite, 97% pure (metals basis) from Alfa Aesar. In addition to real-time monitoring of the gaseous species as a function of time via the FTIR spectrometer built into the continuously circulating reaction system, we also opened the experiment after every fifth run to measure the surface area of a small sample of the catalyst using a commercial, liquid nitrogen-cooled surface area analyzer.

The Experimental System

The experimental system has been described previously (Hill and Nuth 2003) and is shown schematically in Fig. 1. For these experiments, we always used the same gas mixture: 75 torr CO, 75 torr N_2, and 550 torr H_2 measured at room temperature, for a total initial gas pressure of 700 torr. The gas pressure increases as we heat the catalyst to our working temperature, then changes as the CO and H_2 are converted to various products during the course of the reaction. We note that we do not heat the tubing used to circulate the gas in this system, so that in many of the experiments the pressure of water generated via the reactions in the system exceeds the equilibrium vapor pressure of water at room temperature and measurements of the concentration of water in the system therefore reach a plateau at just under 20 torr. Condensation of the excess water vapor throughout the experimental system depletes the initial oxygen in the system and therefore could suppress the formation of CO_2. The FTIR spectrometer records the spectrum of the infrared-active gases in the system at regular intervals, depending on the rate of change we expect for a particular experiment and is set to provide a reasonably continuous record of the CO depletion and CH_4 generation as a function of reaction time for a given experiment.

We are aware that the pressures used in our experiments are much higher than those in the solar nebula and are also aware that this difference could affect the results of our experiments. We would love to duplicate nebular conditions and run our experiments continuously at nebular pressures for several hundred years but such timescales are impractical. On average,

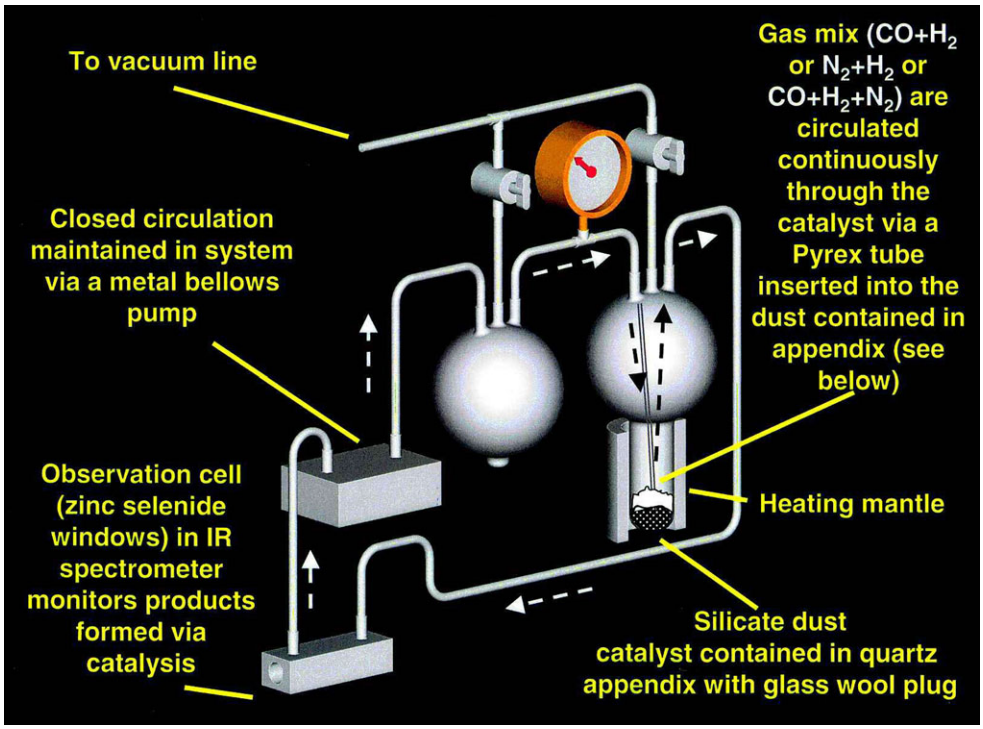

Fig. 1. Three-dimensional drawing of the experimental system used for catalytic experiments. The catalyst is contained in the bottom of a quartz finger (attached to a 2–L Pyrex bulb) that can be heated to a controlled temperature. A Pyrex tube brings reactive gas to the bottom of the finger. The gas passes through the catalyst into the upper reservoir of the bulb and flows through a stainless steel tube at room temperature to a glass-walled observation cell (ZnSe windows) in an FTIR spectrometer. A closed-cycle metal bellows pump returns the sample via a second 2-L bulb and the Pyrex tube to the bottom of the catalyst finger to start the cycle over again. We have 10 identical experimental systems: the total volume of each system is 4.7 ± 0.1 L.

our experiments run for from several days to several weeks. If an average experiment lasts for a week (6.05×10^5s) but should last for a century (3×10^9s) to duplicate conditions found in protostellar nebulae, we can get the same number of reactive CO collisions with our surfaces by increasing the pressure by a factor of $\sim 5 \times 10^3$, from about 10^{-4} to 10^{-3} atmosphere in the nebula to from 0.5 to 5 atmosphere in our experiments. The experiments that we run at about one atmosphere therefore underestimate the number of collisions experienced by an average grain surface in the nebula in 100 yr. Grains could circulate in such nebulae for 10^4 yr or even longer (but at differing temperatures). We will consider pressure to be a proxy for time and will generally ignore its effects on our products in these initial experiments (except as noted in the Discussion) though we do intend to vary pressure in future experiments.

We can try to predict the expected final product distribution that we should see as a function of temperature for our experimental system using a thermodynamic model and our input gas mixture. The final expected product distribution can be seen in Fig. 2. Note that below 723 K, CO is quantitatively converted to methane and water: Above this temperature, methane and water production decrease while the final abundances of CO and CO_2 increase. In addition, N_2 remains virtually unchanged across the entire temperature range with only very low levels of ammonia stable at the lowest temperatures. The abundance of water vapor is above the saturation vapor pressure in all temperature ranges and solid carbon is unstable at all temperatures in the presence of both water vapor and excess hydrogen. While these overall trends are generally correct, the detailed results of our experiments are quite different.

The product distribution in our experiments is complex (Hill and Nuth 2003) and includes a wide range of aromatic and aliphatic hydrocarbons as well as amines, amides, and cyanogens. One should not expect a thermodynamic model to predict such species when, indeed they were not included in the model: this simply demonstrates that a much more complex model would be necessary to account for all of the species experimentally observed. A more serious discrepancy between the thermodynamic predictions and our experimental results is the production of carbonaceous nanotubes (Nuth et al. 2010a, 2010b) at temperatures

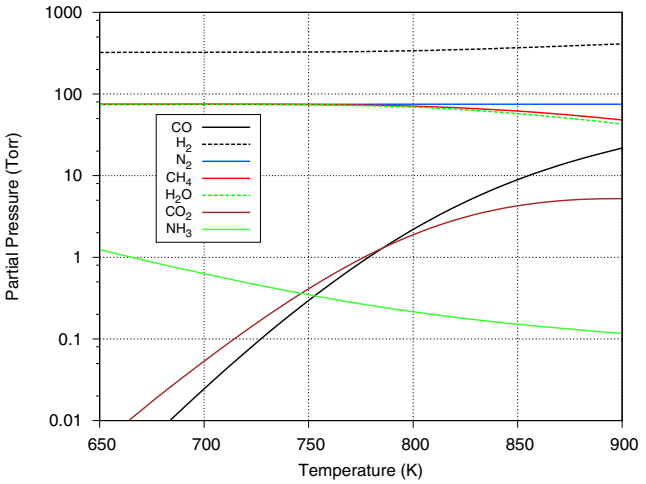

Fig. 2. The equilibrium partial pressures as a function of temperature for an initial mixture consisting of 75 torr of CO, 75 torr of N_2, and 550 torr of H_2 calculated based on the Fischer-Tropsch, Haber-Bosch, Boudouard, and water-gas shift reactions.

above 500 C. The growth of these carbonaceous grains could be the reason why the reaction efficiency of our catalyst increases with use (Nuth et al. 2008) when all reasonable expectations would suggest that its efficiency should decrease. This suggests that a kinetic treatment of this problem may be appropriate provided that we can measure the rate of formation of the solid carbon as well as the relevant gas-phase species.

Measuring Carbon Gas to Solid Branching Ratios

Quantitative measurements of all gases in the system are made by generating synthetic spectra using the high resolution transmission (HITRAN) spectroscopic database (Rothman et al. 2013) and comparing these data with experimentally measured FTIR spectra (Ferguson et al. 2015). These gas species include CO, CO_2, CH_4, C_2H_6, C_2H_2, NH_3, and H_2O. CO is the only source of carbon in the reaction system. Because we do not have a method to directly measure the number of moles of carbon deposited onto the catalyst surface, we measure this quantity indirectly by subtracting the molar quantities of CO, CO_2, CH_4, C_2H_2, and C_2H_6 in each spectrum from the initial number of moles of CO in the system and we assume that the difference was deposited onto the surface of the catalyst. This will be discussed in more detail below. As CO_2, CH_4, C_2H_6, and C_2H_2 constitute the overwhelming majority of the carbonaceous gas-phase products observed in our system, and the quantitative calculation of the gas-phase concentrations from FTIR spectra are accurate to at least 10% or better, we believe that this assumption is reasonable. To complement these measurements, we periodically measured the surface area of the catalyst, as described in the next section: note however that there is not necessarily a direct correlation between the number of moles of carbon solids produced in the reaction and the surface area of the catalyst as the surface area depends on the morphology of the deposited carbon as well as on the quantity.

A more difficult problem in the determination of rate constants or activation energies for these experiments is that the catalyst surface continuously changes during the course of each experimental run. We have previously noted that any surface that we have studied catalyzes the formation of methane from carbon monoxide and that the catalytic activity appears to become more efficient with run number (Nuth et al. 2008). While such changes occur very slowly for some catalysts (e.g., magnesium silicate smokes), the change can be quite rapid for other catalysts as will be seen below. Furthermore, the initial gas/solid carbon branching ratio depends both on the catalyst as well as on temperature, providing a very wide range of experimental parameters that will eventually require study. For this first study, our goal was to understand the major trends in this system with respect to the ratio of carbon atoms incorporated into gas-phase products compared to the fraction of the initial CO incorporated into solids (the gas/solid carbon branching ratio).

EXPERIMENTAL RESULTS

In the supporting information, we present an example of the spectral changes that occur throughout a typical experimental run together with examples of the analyses of the gas-phase abundances of individual infrared-active constituents such as CO, CO_2, CH_4, and H_2O taken from an experimental run at 873 K using a magnetite catalyst. In the tables that follow, we list the gas-phase abundances derived from the spectral analyses of all of the experiments used to generate the plots seen in the rest of the paper. In particular, we tabulate the time-dependent total pressure (in units of torr) as well as the partial pressures of H_2O, CO_2, CO, CH_4, C_2H_6, C_2H_2, and the fraction of the initial carbon (initially in CO) deposited as a solid. Finally, we show plots of the rate of CO decay for surface-mediated reactions at 873 K and at 773 K from which we derive the order of the reaction at each temperature.

Surface Area and Morphology of the Catalyst

Surface-mediated reactions can occur at active catalytic sites on almost any grain surface (Hayatsu and

Table 1. Variation of catalyst surface area with run number.

Catalyst	Surface area (m^2 g^{-1})
Initial magnetite sample	7.41
Magnetite, 5 runs at 450 °C	19.65
Magnetite, 10 runs at 450 °C	33.95
Magnetite, 15 runs at 450 °C	35.31
Magnetite, 20 runs at 450 °C	49.46

Anders 1981; Hill and Nuth 2003) and we have previously demonstrated that the deposition of refractory carbonaceous material on grain surfaces can actually enhance the rate of such reactions (Nuth et al. 2008). We had made the simple assumption that the carbonaceous coating grew to cover the surface of the underlying catalyst, leaving an outer coating that completely and uniformly covered the original grain. Such "grain varnishes" or refractory organic residues have frequently been described in the past as the result of ultraviolet or radiation processing of ices containing simple organic precursors such as CH_4, CH_3OH, CH_2O, and NH_3 (Ashbourn et al. 2007; Sandford 2005). It seemed natural to assume that a similar morphology would result from surface-mediated processes. That assumption is incorrect.

In these studies, we used a Quantichrome Nova E series surface area analyzer and the BET technique (Brunauer et al. 1938) with N_2 as the adsorbed gas to measure the area of our initial pure magnetite catalyst, as well as small samples of the catalyst that had been used for 5, 10, 15, and 20 experimental runs. We found that the area of our catalyst increased significantly at each measurement. This implies that the area increases during each individual run as well making quantification of the reaction kinetics as a function of the catalytic surface area an interesting challenge that we will tackle in future work. The results of these measurements for an initially pure magnetite catalyst are given in Table 1. As can be seen, the active catalytic surface area more than doubled relative to the surface area of the original magnetite catalyst within the first five experimental runs, then increased to more than four times the initial magnetite surface area after 10 runs, and to more than six times the original area after 20 experiments. It is highly unlikely that the catalyst remains pure magnetite as its surface area increases.

Unfortunately, these results should be taken as lower limits to the actual increase in surface area that occurred during these experiments. As we began to quantitatively measure the reaction rates per unit surface area of catalyst, we became aware that the rates did not scale by the area of the catalyst as we had expected. Instead, the rate for iron powders compared

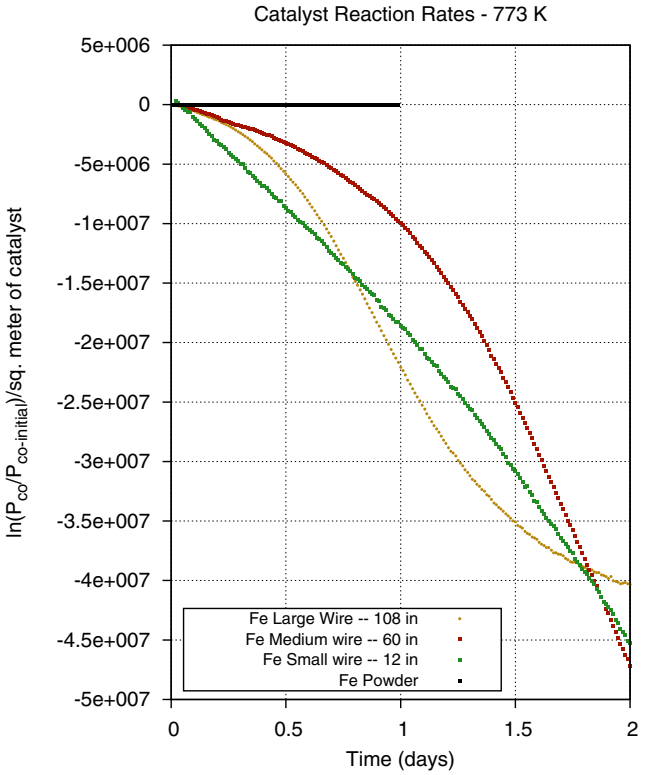

Fig. 3. A plot of the relative loss of CO as a function of time scaled to the surface area of the catalyst. Note that the CO loss rate per unit surface area is within family when samples of iron wire were used as catalysts, but is dramatically slower when bulk iron powder is used, indicating that only a small fraction of the available surface area of the powder plays a part in catalyzing the overall reaction.

to the rate for several lengths of iron wires shown in Fig. 3 indicated that most of the iron powder was not seen by the reactive gas mixture. The experimental system shown in Fig. 1 was set up as a fluidized bed reactor in which the gas injected at the bottom of the catalyst bed "liquefies" the very fluffy iron silicate smokes that we first tested as catalysts. In such a system, the gas interacts freely with the entire catalyst bed. Use of the much denser iron, hematite, or magnetite powders in this system eliminates the fluidity of the catalyst at the gas flow rates available in our system, and even though we thought that the gas permeated the entire reaction bed, it is obvious from Fig. 3 that a significant portion of the iron powder catalyst did not participate in the reaction. While this does not change the product distribution of the reactants we are reporting here, it certainly affects measurements of the reaction kinetics and means that measurements of the surface area per gram of an iron or magnetite powder catalyst, measured for a randomly drawn sample of the bulk material, averaged the increased surface area of active grains with a larger

quantity of grains that had minimal interaction with the gas.

Even this lower limit for the rapid increase in the surface area of the catalyst was very difficult to explain based on our previous experiments and with our ingrained assumptions concerning the morphology of the deposited coating. Previous analyses of the coating on iron silicate smokes with initial surface area ~125 m^2/g and a total mass less than 5 g showed that after 20 runs, the grains were 10% by mass carbon and 0.2% by mass nitrogen (Gilmour et al. 2002). Increasing the surface area of our catalyst by a factor of 6 would require more than doubling the average radius of the 325 mesh magnetite catalyst and would require much more than the available quantity of carbon in the system to accomplish this increase. Based on our previous work, we would expect that much less than a gram of carbon deposition occurs (total on all grains in the system) over 20 runs and we know that a significant fraction of the available carbon is converted into CO_2, CH_4, and other volatile organic species via the overall reaction (Nuth et al. 2008). This does not leave enough mass to coat the initial magnetite grains to sufficient thickness to increase their surface area by factors of 4 or more. Continuous carbonaceous coatings on the catalytic surfaces can therefore be ruled out by these measurements: a more complex surface morphology is required.

In previous experiments conducted at 873 K using a graphite catalyst, we have shown the formation and growth of carbon nanotubes (Nuth et al. 2010b), essentially a thin string of carbon with a very high surface area per unit mass. A TEM image of these deposits is shown in Fig. 4 to illustrate the very large surface area possible for such morphologies that we had believed were unique to experiments using graphitic catalysts and their large reservoir of potentially reactive carbon. We had never seen evidence for nanotube formation at temperatures less than 823 K for any other catalyst, including in both SEM analyses as well as in electron diffraction analyses of lower temperature grain coatings. In our previous SEM images, the surface always appeared to be "lumpy"—which we attributed to grain clumping and other macroscopic features produced during the reaction.

Higher resolution SEM images of iron silicate smokes used as catalysts at 873 K tell a very different story as can be seen in Fig. 5. It appears that active regions on the surface of the catalyst initially promote carbon deposition in the local area. However, rather than spreading uniformly over the surface of the grains, the carbon deposit also begins to grow away from the catalyst surface. While in some ways this initially appears to resemble VLS (vapor–liquid–solid) growth

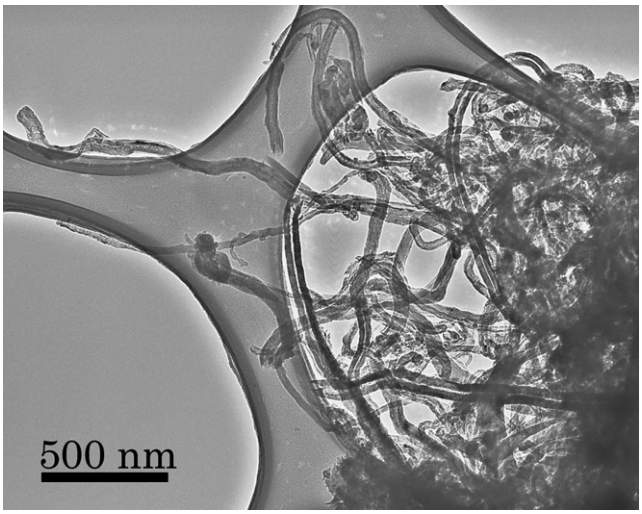

Fig. 4. Surface-mediated reactions produce very high surface to volume deposits on graphite grains used as catalysts as can be seen in this TEM image of carbon nanotubes grown from our standard gas mixture (75 torr CO, 75 torr N_2, 550 torr H_2) at 873 K (Nuth et al. 2010b). We had previously believed that such extensive nanotube growth was unique to graphitic catalysts and was due to the ready supply of carbon atoms available from the graphite grains themselves.

along a crystalline "*c*-axis," the resultant deposit is neither crystalline nor is it a smooth needle or whisker: In fact, it is rather clumpy and quite irregular. It also appears that much, if not all, of the deposited carbon is capable of promoting additional surface-mediated reactions and further carbon deposition much as we had observed when using the graphite catalyst. The newly deposited carbon does not appear to thicken the nanotubes themselves, but instead appears to cause them to lengthen. Based on experiments on the formation and growth of nanotubes (Nuth et al. 2010b), we know that carbon atoms are relatively easily mobilized from such initial condensates to form longer nanotubes—another similarity to VLS growth. It is possible that once such tubes begin to form, the chemical composition of the original catalyst becomes increasingly less important with time.

The formation of filamentous carbon deposits is one possibility that may explain both the dramatic increase in specific surface area and increased catalytic activity. Such filamentous carbon is known to occur in carburizing and reducing atmospheres in the 400–800 °C range. Such deposits have been known for some time; one of the first reports of such deposits was made after observations of the reaction of carbon monoxide with iron oxide on the brickwork in a blast furnace (Davis et al. 1953). Schultz et al. (1961) found such structures while studying Fischer-Tropsch and methanation catalysts and termed the deposits

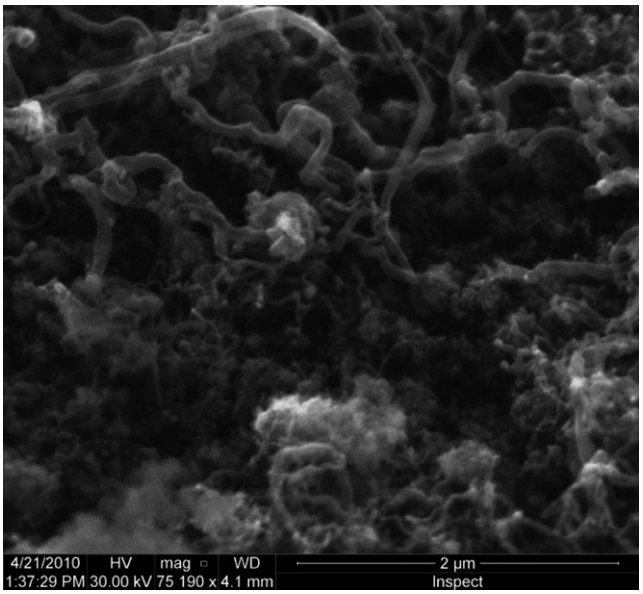

Fig. 5. Typical SEM image of an iron silicate sample after 16 heating cycles at 873 K. The conditions of SEM observation are as follows: accelerating voltage is 30 kV in high vacuum, pressure is 0.1 mtorr, temperature is 298 K, and the sample is sputter coated with Au-Pd at an emission current of 100 mA. The image has been magnified by a factor of 75,000. CO is the only source of carbon available for the growth of nanotubes in these experiments.

"carbon-expanded iron." Schultz et al. (1961) suggested that, under certain conditions, the carbon deposition broke the bulk metal into finer particles. The carbon would grow into filaments that would keep the metal particles from agglomerating, thereby making the metal more accessible to reactant gases. Schultz et al. (1961) noted the unexpected catalytic activity per gram of material after the growth of these carbon-expanded iron filaments. Such behavior may be responsible for the increased catalytic activity noted with the current catalysts where reaction rates increase with successive runs.

In industrial processes, such deposits can occur on the steel reactor walls, causing harmful effects. One particular growth of carbon, called "metal dusting," causes the corrosion of vessel walls, resulting in a dust of graphite and small metal particles (Grabke 2003). Both the filamentous carbon and metal dusting growth occur with metals that absorb carbon, e.g., iron, nickel, and cobalt. Carbon is absorbed and transported within the metal due to a gradient in carbon activity. In fact, the diffusion of carbon in the catalyst particle is thought to be the rate-determining step in the reaction sequence because there is very close agreement between activation energies for filament growth and those for diffusion of carbon through the metals (Baker 1989).

The formation of filamentous carbon deposits on metal particles is outlined in six steps given by Bonnet et al. (2003). These steps include (1) the decomposition of hydrocarbons on the metal surface and supersaturation of the metal with absorbed carbon; (2) the nucleation and growth of cementite, Fe_3C; (3) carbon diffusion becomes impeded through the cementite layer and hinders further transfer from the gas phase; (4) graphite then begins to precipitate on the cementite surface, reducing the activity of carbon at the graphite/cementite interface thus making cementite unstable and causing it to decompose into carbon and iron; (5) these free carbon atoms attach to the basal planes of graphite that grow into the cementite while the iron atoms agglomerate to form small particles and finally; (6) these small particles are able to act as catalysts for further carbon deposition and growth. While these steps outline the growth of filamentous carbon with metallic iron, Bonnet et al. (2003) has proposed a new mechanism whereby iron oxides can also form such filamentous structures by being converted directly to cementite without having metallic iron as an intermediate phase. This filamentous carbon should thus be able to form with iron oxide mixtures as well as on metallic iron covered with oxide layers. Thus far, the available experimental evidence seems to support the formation of this filamentous carbon and further experiments will be focused on imaging and chemical analyses of such deposits using high-resolution microscopy to investigate this possibility.

Gas/Solid Branching Ratios

As noted in the Introduction, synthetic spectra generated using the HITRAN database can be used along with measured FTIR spectra to quantify the majority of the carbon-containing, gaseous species in our experiments. Therefore, the fraction of the initial carbon available in the original carbon monoxide feedstock deposited on the grain surface can be calculated from this information. Tables of gas-phase abundances for all experimental runs, examples of synthetic spectra generated by the HITRAN program compared to experimental spectra, and plots of the reaction of CO as a function of time for several temperatures and catalysts are contained in the supporting information. Before considering these data, some insight may be gained by further considering what species are predicted to be present in an equilibrium mixture based on a typical initial gas charge. This information may be useful in assessing catalyst selectivity to the methanation reaction or the formation of deposited carbon and hydrocarbons.

Table 2. Computed equilibrium partial pressures of experimental gases.

Temperature	400 °C	500 °C	600 °C
CO	0.029	1.237	14.21
H_2	324.16	332.8	387.4
N_2	74.68	74.88	74.95
CH_4	75.00	72.70	55.81
H_2O	74.89	71.58	50.82
CO_2	0.064	1.11	4.991
NH_3	0.678	0.283	0.133
Total pressure	549.5	554.5	588.3

All computations were made with starting mixtures of 75 torr carbon monoxide, 75 torr nitrogen, and 550 torr hydrogen at the noted temperatures. All pressures are given in torr.

A sample of four competing reactions that can occur under the conditions of the experiments was given in the Introduction. To compute the equilibrium, gaseous concentrations with such multiple reactions, the minimization of Gibbs free energy technique using Lagrange multipliers was used (White et al. 1958) with a starting gas mixture of 75 torr carbon monoxide, 75 torr nitrogen, and 550 torr hydrogen. The results of these calculations for the major reactant and product gases are shown as a function of temperature in Fig. 2 and in Table 2.

As shown in Table 2, the formation of methane is favored at lower temperatures with virtually all of the carbon monoxide consumed and converted to methane. As the temperature increases, the reaction shifts, less methane is predicted to be formed and there is residual carbon monoxide as well as some carbon dioxide in the equilibrium mixture. As the consumption of carbon monoxide is used to determine when to terminate the experiments, it is important to note that not all of the carbon monoxide may be consumed at the higher system temperatures. Because of the low system pressure (compared to those used in the industrial Haber-Bosch process), only a small amount of ammonia is predicted to be formed and larger, equilibrium amounts of ammonia are also favored at the lower temperatures. In several experiments, it is common to form ~50–60 torr of methane; in these cases, it is clear that the overall reaction at equilibrium favors the methanation reaction and the selectivity to form condensed hydrocarbons is low.

Figure 6 shows the measured carbon gas/solid fraction for a magnetite catalyst as a function of time and run number for a series of experiments conducted at 773 K. Approximately 25% of the carbon in the initial CO is deposited onto the surface of the Fe_3O_4 catalyst by the end of each experimental run while the bulk of the carbon remains as gas-phase CO, CO_2, CH_4, and C_2H_6. Note the anomalous behavior at the

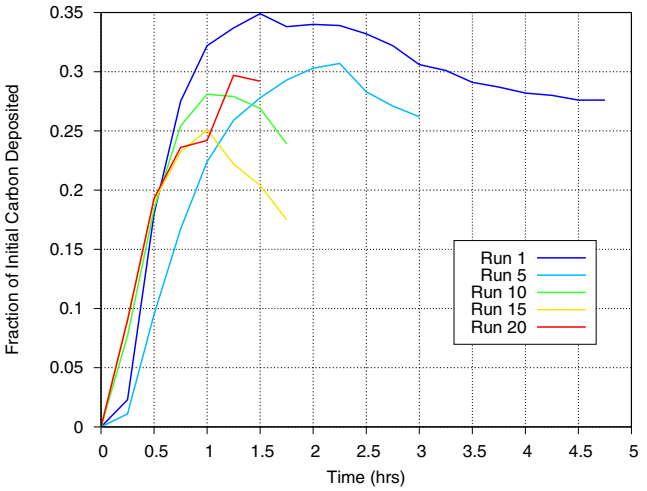

Fig. 6. The fraction of the available carbon from CO that is deposited onto a magnetite catalyst at 773 K as a function of time during various experimental runs. Earlier runs generally deposit a larger fraction of the available carbon as solids.

start of runs 1 and 5. We always measure the initial CO concentration and perform quantitative measurements using the synthetic spectra generated using the HITRAN database at the temperature of the FTIR cell (room temperature) and the measured total system pressure. The anomaly results because there is a rapid rise in total system pressure when heat is applied to the catalytic "finger" thus increasing the concentration of gas-phase species in the FTIR cell.

For the first measurement made at the start of a run, the pressure will be 700 torr (by design at room temperature). However, because the catalyst finger is now being heated to 773 K (for the data shown in Fig. 6) as we start the system, the temperature of the finger will be somewhat higher, thus increasing the pressure throughout the closed system. A higher pressure in the system will lead to an artificial increase in the gas-phase abundance of carbon as determined from comparison between synthetic and measured spectra for the second and all subsequent measurements until the surface-mediated reactions begin to deposit carbon onto the grains or until fewer moles of gas-phase species are formed as reaction products. If carbon deposition or the overall reaction rates are slow, the negative anomaly will persist for some time. For faster rates of deposition, carbon will be taken out of the gas phase more rapidly and increasing gas pressure can be compensated for by carbon deposition. Note that in Fig. 6, the anomaly is pronounced for run 1, less pronounced in run 5, and much less obvious in runs 10, 15, and 20. As the catalytic finger was heated at the same rate for each experimental run, these data imply either that the rate at which carbon is deposited onto

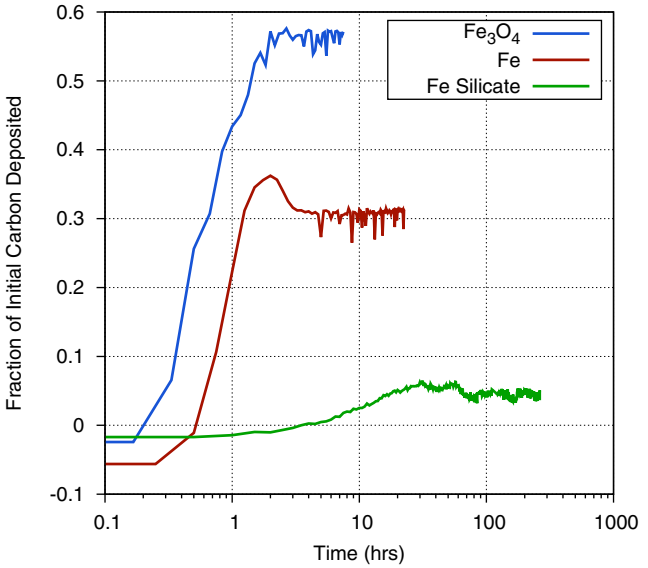

Fig. 7. The fraction of the available carbon from CO deposited onto a magnetite, iron, or iron silicate catalyst during the initial experimental run at 873 K as a function of time shows a very wide range in gas/solid branching ratio.

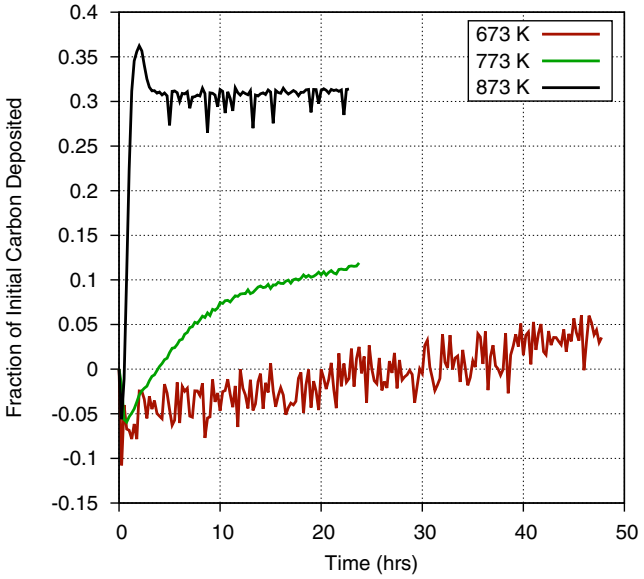

Fig. 8. The fraction of the carbon available from CO deposited onto an iron catalyst as a function of time for several different temperatures during the first experimental run with a fresh catalyst.

the surface of the catalyst at the beginning of each experiment increased as a function of run number or that the overall reaction rate increased. Thus, the more carbon that has already been deposited onto the magnetite surface, the faster carbon is deposited onto that surface in subsequent experiments.

Figure 7 shows the different initial rate and gas/solid fraction for carbon deposition onto iron, magnetite, and amorphous iron silicate smokes at 873 K. Fe_3O_4 very efficiently converts the initial C in the CO feedstock into a carbonaceous deposit, as compared to pure Fe or the amorphous silicate smokes. Figure 7 also demonstrates the considerable differences among catalysts in the fraction of carbon deposited onto grain surfaces versus the fraction that is converted into gas-phase products. At 873 K, nearly 60% of the CO exposed to a magnetite catalyst is deposited onto the surface, whereas only 30% of the carbon exposed to an iron catalyst is converted into a carbonaceous deposit. Even at high temperatures, where the Boudouard reaction should become much more important, much less CO is converted into a solid on the amorphous iron silicate catalysts. The effect of temperature is more dramatically illustrated in Fig. 8, where the fraction of CO deposited onto an iron catalyst surface at three different temperatures varies from 0.3 at 873 K to ~0.12 (accounting for the anomaly discussed above) at 773 K, and down to ~0.05 at 673 K. Obviously, for a pure Fe catalyst, the branching ratio of the carbon deposited onto the grain surface compared to the carbon incorporated into volatile compounds is a very strong function of temperature. Higher temperature yields fewer volatiles. This is consistent with the general trend in the Boudouard reaction but is not consistent with thermodynamic predictions of the instability of free carbon in the presence of excess hydrogen.

DISCUSSION

We started these experiments with the intention of measuring the gas/solid product branching ratio as well as the rate of surface-mediated reactions on several different catalysts as a function of temperature and run number under the assumption that roughly similar quantities of carbonaceous materials would be deposited on all of the catalysts at a given temperature as a function of time. This is obviously not the case. In fact, we have seen that the rate of carbon deposition varies significantly as a function of run time. Thus, the previous reaction history of the catalyst also has a significant role in determining its reactive efficiency as well as the overall rate and activation energy of the reaction. As noted above we found that a significant, but not well quantified fraction of our powder catalysts were not functional participants in the overall reactions. However, if we assume that approximately the same fraction of each catalyst was active for runs at each temperature, we can make some very qualitative statements concerning the kinetics of the overall

surface-mediated reaction CO + N_2 + H_2 => products. In future experiments, we will make quantitative measurements of the reaction rate for this overall reaction per unit surface area for each catalyst.

For temperatures of ~773 K or less, the reactions follow first-order kinetics in CO at least for the initial portion of the first run with a Fe_3O_4 catalyst. This implies that the initial dissociative adsorption of CO on the active catalytic site is the rate controlling step, as was previously noted by Kress and Tielens (1999). However, in experiments at ~873 K, the reaction kinetics appears to be transitioning from first to second order in CO even for the first run using a Fe_3O_4 catalyst. This would indicate that the reaction set dominated by the adsorption of CO onto magnetite at lower temperatures transitions to an overall reaction increasingly dominated by some variation of the Boudouard reaction (2CO=>C + CO_2) at higher temperatures. Note that in the presence of excess hydrogen, the CO_2 formed via the Boudouard reaction can react to reform CO + H_2O (which has a natural tendency to condense out on the inside surface of our reaction system) and would thus tend to push the reaction to deposit even more carbon onto the catalytic surface. This would agree with our observations that a greater fraction of the initial CO is deposited onto the catalyst surface as carbonaceous solids at higher temperatures. However, at the lower total pressures of a nebular environment, a second-order reaction's efficiency should be greatly decreased and the Boudouard reaction might not play any significant role in the formation of the initial carbonaceous solids until much higher temperatures (e.g., >>875 K). Experiments that vary the initial absolute CO concentration will be carried out in the future to test this hypothesis.

We already know that the morphology of the carbonaceous solid is temperature-dependent: carbon nanotubes are formed at 873 K, but are not readily observed at lower temperatures (Nuth et al. 2010b). Nanotubes are highly ordered aromatic carbon. Carbonaceous deposits formed at lower temperatures are less aromatic and probably contain more nitrogen, oxygen, and hydrogen than do coatings formed at higher temperatures based on previous studies (Gilmour et al. 2002). We do not yet know if the composition of the initial carbonaceous deposit depends strongly on the specific catalyst used in the experiments, if such deposits contain metal atoms from these catalysts, or how the composition of the average deposit might change as the catalyst becomes coated, the filamentous carbon grows, and the primary catalytic surface transitions from the inorganic grain species to the carbonaceous deposit. We speculate that no matter the underlying grain surface, as the carbonaceous deposit increases, its composition and catalytic efficiency should approach a state whose nature is more dependent on temperature than on any initial conditions. Unfortunately, because the rates of surface-mediated reactions greatly decrease with temperature, it will take a long time to investigate this hypothesis. Table 3 shows the time that we estimate will be required to carry out both a single experiment and 20 consecutive runs at specific temperatures based on our current data.

Table 3. Estimated experimental run times as a function of temperature.

Temperature	Time/run	20 runs
873 K	0.5 weeks	2.5 months
773 K	~1 week	5 months
673 K	3 weeks	14 months
573 K	6 weeks	28 months
473 K	12 weeks	56 months
373 K	24 weeks	111 months

Implications for Nebular Dust

Our experiments indicate that macroscopic carbon particles, many hundreds—or even thousands—of nanometers in length and quite irregular in shape, could form at least on the surfaces of both magnetite and graphite grains, and probably on other surfaces as well and this could have several consequences. First, such carbon-rich growths could at least partially replenish presolar graphite-like dust previously destroyed in high-temperature nebular shocks, lightning strokes, or in close proximity to the early sun. While we know that a large fraction of presolar silicate grains were processed in the nebula to produce the much larger dust particles found in meteorite matrix, presolar carbon dust must have experienced similar heating processes, though no quantitative measure of such processing is yet available in the literature. However, while silicates are converted into liquid droplets or vapor at high temperatures—and silicate vapor can recondense—carbon must be converted into CO or CO_2 at high temperatures in the oxygen-rich solar nebula or when in direct contact with silicate grains. Surface-mediated reactions would be a significant pathway to convert such gases back into the solid carbon species found in meteorites.

An interesting possibility, if such processes occur on the surfaces of larger (mm scale) silicate and metallic grains in the nebula, is that such growth could act much in the same manner as do fresh snowy condensates on the surfaces of the larger ice grains in Saturn's rings. An example of this is shown in Fig. 9, where a section of iron wire is compared before and after use as a catalyst for a single experimental run. Such fluffy grain coatings could damp out the momentum in gently colliding particles, changing the coefficient of restitution and

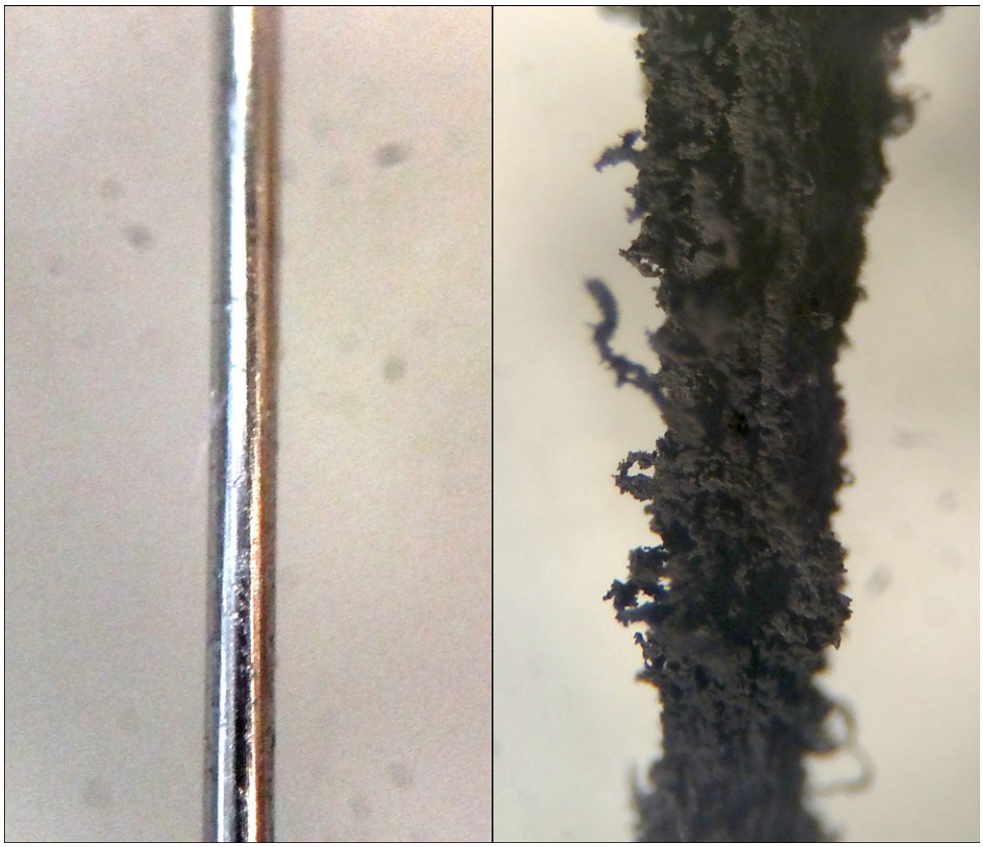

Fig. 9. A microscope image of a section of iron wire used in the experiments (0.009 inches in diameter) shown at the same scale before (left) and after (right) it served as the catalyst for a single experimental run of CO + N_2 + H_2 => products at 873 K.

promoting grain–grain sticking (Hatzes et al. 1988; Dilley and Crawford 1996). Surface-mediated reactions would happen fastest in the higher temperature, higher pressure regions of the inner solar nebula, just where chondrules, CAIs, and other macroscopic meteoritic components are also forming. Under such circumstances, the solid carbonaceous products would tend to be more graphitic and could even be similar to the stacked-cup nanotubes that we have observed previously (Nuth et al. 2010b). If some of these refractory surfaces served as catalytic sites for the growth of filamentous "whiskers," then such surface growth could also promote the aggregation of these larger meteoritic components. In fact, at least one study has reported an association between carbon nanotubes and CAIs (Fries and Steele 2008). Could such carbonaceous growth be the glue that promoted the aggregation of meteorite parent bodies in the high temperature inner nebula?

CONCLUSIONS

Surface-mediated reactions in natural protostellar environments are much more complex than previously believed. Even the highly simplified experimental model system presented here is much more complex than we initially expected but is still far from capable of predicting the wide range of products formed via surface-mediated processes in protostellar nebulae. The ratio of solid carbon deposited onto grain surfaces versus the volatiles released back into the gas phase depends strongly on temperature and time, on the properties of the initial catalyst (composition and surface area), and on the previous history of the catalyst, e.g., the run number, used as a proxy to track the relative amount of previously deposited carbon. To make things even more interesting, the surface area of all of the catalysts that we have studied increase with time. The surface-mediated reaction rate depends on run number and may change as carbon deposits on or even within grain surfaces. In addition, the order of the overall reaction appears to be a function of temperature. At lower temperatures, the reaction depends linearly on the concentration of CO, indicating that the reaction rate depends on the adsorption of CO at reactive sites on the catalyst. At higher temperatures, the overall reaction rate approaches second order, indicating a more important role for the Boudouard reaction (the disproportionation of CO into

C + CO_2). However, as this reaction is both pressure-(second-order kinetics) as well as temperature-dependent and as the CO concentration in protostellar nebulae is considerably less than that in our experiments, such reactions might not become important in nebular environments until much higher temperatures are reached.

For the primitive solar nebula, surface-mediated reactions might provide a solution for a problem that modern chemical models of nebular processes do not address; namely, the conversion of large quantities of CO and CO_2 generated by high-temperature reactions under oxidizing conditions back into solid carbonaceous species that can be more easily incorporated into planetesimals. Planetesimal accretion could also be enhanced by the formation of fibrous, nanotube-like growth on the surfaces of larger refractory meteoritic components such as chondrules or CAIs. Such surface coatings could dampen the energy of grain–grain collisions and significantly increase their sticking coefficient in the higher temperature inner nebula. Much more work is needed to unravel the effects of competing chemical processes on grain surfaces in order to model their possible impact on nebular chemistry and dynamics.

Acknowledgments—The authors thank the two anonymous reviewers of this manuscript for their very helpful and constructive comments. We also thank the associate editor, Dr. Scott Sandford, for his help and suggestions for improving the presentation of our results.

Editorial Handling—Dr. Scott Sandford

REFERENCES

Anders E., Hayatsu R., and Studier M. H. 1974. Interstellar molecules: Origin by catalytic reactions on grain surfaces? *The Astrophysical Journal* 192:L101–L105.

Ashbourn S. F. M., Elsila J. E., Dworkin J. P., Bernstein M. P., Sandford S. A., and Allamandola L. J. 2007. Ultraviolet photolysis of anthracene in H_2O interstellar ice analogs: Potential connection to meteoritic organics. *Meteoritics & Planetary Science* 42:2035–2041.

Baker R. T. K. 1989. Catalytic growth of carbon filaments. *Carbon* 27:315–323.

Bonnet F., Ropital F., Berthier Y., and Marcus P. 2003. Filamentous carbon formation caused by catalytic metals particles from iron oxide. *Materials and Corrosion* 54:870–880.

Boynton W. V. 1985. Meteoritic evidence concerning conditions in the solar nebula. In *Protostars and planets II*, edited by Black D. C. and Mathews M. S. Tucson, Arizona: The University of Arizona Press. pp. 772–787.

Brunauer S., Emmett P. H., and Teller E. 1938. Adsorption of gases in multimolecular layers. *Journal of the American Chemical Society* 60:309–319.

Davis W. R., Slawson R. J., and Rigby G. R. 1953. An unusual form of carbon. *Nature* 171:756.

Dilley J. P. and Crawford D. 1996. Mass dependence of energy loss in collisions of icy spheres: An experimental study. *Journal of Geophysical Research* 101:9267–9270.

Draine B. T. and Lee H. K. 1984. Optical properties of interstellar graphite and silicate grains. *The Astrophysical Journal* 285:89–108.

Fegley B. 1999. Chemical and physical processing of presolar materials in the solar nebula and the implications for preservation of presolar materials in comets. *Space Science Reviews* 90:239–252.

Fegley B. and Hong Y. 1998. Experimental studies of grain catalyzed reduction of CO to methane in the solar nebula. *Eos* 79:S361–362.

Ferguson F. T., Johnson N. M., and Nuth J. A. III. 2015. On the use of Fourier transform infrared spectroscopy and synthetic calibration spectra to quantify gas concentrations in a Fischer-Tropsch catalyst system. *Journal of Applied Spectroscopy* 69:1157–1169.

Ferrante R. F., Moore M. H., Nuth J. A., and Smith T. 2000. Formation of carbon compounds by catalytic conversion of CO on laboratory grain analogs containing iron. *Icarus* 145:297–300.

Fries M. and Steele A. 2008. Graphite whiskers in CV3 meteorites. *Science* 320:91–93.

Gilmour I., Hill H. G. M., Pearson V. K., Sephton M. A., and Nuth J. A. 2002. Production of high molecular weight organic compounds on the surfaces of amorphous iron silicate catalysts: Implications for organic synthesis in the solar nebula (abstract #1613). 33rd Lunar and Planetary Science Conference. CD-ROM.

Grabke H. J. 2003. Metal dusting. *Materials and Corrosion* 54:736–746.

Hatzes A. P., Bridges F. G., and Lin D. N. C. 1988. Collisional properties of ice spheres at low impact velocities. *Monthly Notices of the Royal Astronomical Society* 231:1091–1115.

Hayatsu R. and Anders E. V. 1981. Organic compounds in meteorites and their origins. *Topics in Current Chemistry* 99:1–37.

Hill H. G. M. and Nuth J. A. 2003. The catalytic potential of cosmic dust: Implications for prebiotic chemistry in the solar nebula and other protoplanetary systems. *Astrobiology* 3:291–304.

Huss G. R., Keil K., and Taylor G. J. 1981. The matrices of unequilibrated ordinary chondrites: Implications for the origin and history of chondrites. *Geochimica et Cosmochimica Acta* 45:33–51.

Kerridge J. 1989. Interstellar molecules in meteorites. In *International Astronomical Union. Symposium 135: Interstellar Dust*, edited by Allamandola L. J. and Tielens A. G. G. M. Dordrecht, the Netherlands: Kluwer Academic Publishers. pp. 383–388.

Kerridge J. F. 1999. Formation and processing of organics in the early solar system. *Space Science Reviews* 90:275–288.

Kress M. E., and Tielens A. G. G. M. 2001. The role of Fischer-Tropsch catalysis in solar nebula chemistry. *Meteoritics & Planetary Science* 36:75–91.

Mathis J. S., Rumpl W., and Nordsieck K. H. 1977. The size distribution of interstellar grains. *The Astrophysical Journal* 217:425–433.

Nuth J. A., Rietmeijer F. J. M., and Hill H. G. M. 2002. Condensation processes in astrophysical

environments: The composition and structure of cometary grains. *Meteoritics & Planetary Science* 37: 1579–1590.
Nuth J. A., Johnson N. M., and Manning S. 2008. A self perpetuating catalyst for the production of complex organic molecules in protostellar nebulae. *The Astrophysical Journal* 673:L225–L228.
Nuth J. A., Johnson N. M., Meshik A., and Hohenberg C. 2010a. Trapping of planetary noble gases during the Fischer-Tropsch-type synthesis of organic materials (abstract #1232). 41st Lunar and Planetary Science Conference. CD-ROM.
Nuth J. A., Kimura Y., Lucas C., Ferguson F. T., and Johnson N. M. 2010b. The formation of graphite whiskers in the primitive solar nebula. *The Astrophysical Journal Letters* 710:L98–L101.
Nuth J. A., Johnson N. M., and Hill H. G. M. 2014. CO self-shielding as a mechanism to make ^{16}O-enriched solids in the solar nebula. *Challenges* 5:152–158.
Rothman L. S., Gordon I. E., Babikov Y., Barbe A., Brenner D. C., Bernath P. F., Birk M., Bizzocchi L., Boudon V., Brown L.R., Campargue A., Chance K., Cohen E.A., Coudert L.H., Devi V.M., Drouin B.J., Fayt A., Flaud J.-M., Gamache R.R., Harrison J.J., Hartmann J.-M., Hill C., Hodges J.T., Jacquemart D., Jolly A., Lamouroux J., Le Roy R.J., Li G., Long D.A., Lyulin O.M., Mackie C.J., Massie S.T., Mikhailenko S., Müller H.S.P., Naumenko O.V., Nikitin A.V., Orphal J., Perevalov V., Perrin A., Polovtseva E.R., Richard C., Smith M.A.H., Starikova E., Sung K., Tashkun S., Tennyson J., Toon G.C., Tyuterev Vl.G., and Wagner G. 2013. The HITRAN2012 molecular spectroscopic database. *Journal of Quantum Spectroscopy and Radiative Transfer* 130:4–50.
Sandford S. A. 2005. Organic synthesis in space. In *Astrophysics of life, Space Telescope Institute Symposium Series 16*, edited by Livio M., Reid N., and Sparks W. Cambridge, UK: Cambridge University Press. pp. 54–66.
Schultz J. F., Karn F. S., Anderson R. B., and Hofer L. J. E. 1961. A new type of catalyst—carbon—expanded iron. *Fuel* 40:181–192.
White W. B., Johnson S. M., and Dantzig G. B. 1958. Chemical equilibrium in complex mixtures. *Journal of Chemical Physics* 28:751–755.

SUPPORTING INFORMATION

Additional supporting information may be found in the online version of this article:

Data S1: Example experimental FTIR spectra.